Proceedings of ASME Turbo Expo 2011
GT2011
June 6-10, 2011, Vancouver, British Columbia, Canada

GT2011-46483

NEGATIVE STIFFNESS IN GAS TURBINE LEAF SEALS

Ingo H. J. Jahn*
Transmissions, Structures & Drives
Rolls-Royce plc.
Derby, DE24 8BJ, UK
ingo.h.jahn@rolls-royce.com

Andrew K. Owen
Department of Engineering Science
University of Oxford
Oxford, OX1 3PJ, UK

Gervas Franceschini
Transmissions, Structures & Drives
Rolls-Royce plc.
Derby, DE24 8BJ, UK

David R. H. Gillespie*
Department of Engineering Science
University of Oxford
Oxford, OX1 3PJ, UK
david.gillespie@eng.ox.ac.uk

ABSTRACT

The stiffness of contacting shaft seals such as brush seals and leaf seals is a required characteristic to accurately predict their performance and life in the gas turbine engine. This paper describes the results of a test campaign in which a series of eccentric rotor excursions are applied at low rotational speed and engine representative pressure differences to characterise the behaviour of a prototype leaf seal. A phenomenon that may best be described as negative seal stiffness is reported. Here, the displacement of the seal rotor to an eccentric position causes a resultant force, which, rather than trying to return the rotor to a central position, acts to amplify its displacement. These data were used to develop an empirical model of the seal behaviour. It was possible to model the negative stiffness phenomenon and show that it is caused by a combination of two effects: the inherent mechanical stiffness of the leaf pack, and the aerodynamic stiffness of the seal. The latter is caused by the pressure distribution and changes in the flow field through the leaf pack as a result of the displacement of the rotor.

*Corresponding authors.

NOMENCLATURE

δ rotor eccentricity, mm
$F_{Inertia}$, F_I inertia force, N
F_{Net} net force acting on rotor, N
$F_{Pressure}$, F_P pressure force, N
$F_{Stiffness}$, F_S stiffness force, N
F_T total force, N
N number of elements
P_D gauge downstream pressure, MPa
P_U gauge upstream pressure, MPa
p_1 mechanical stiffness coefficient
q_0, q_1 pressure force coefficient
r_0, r_1 inertia force coefficient
t time, s
θ angular position, rad
x_g local gap, mm
x_0 mean gap, mm

INTRODUCTION

The need for improved secondary air-system sealing in gas turbines is well known. A detailed discussion of this was presented by Ferguson et al. [1] and Hendricks et al. [2] amongst

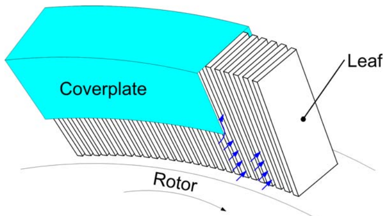

Figure 1. Leaf Seal

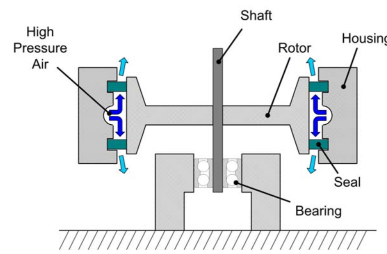

Figure 2. Facility cross section

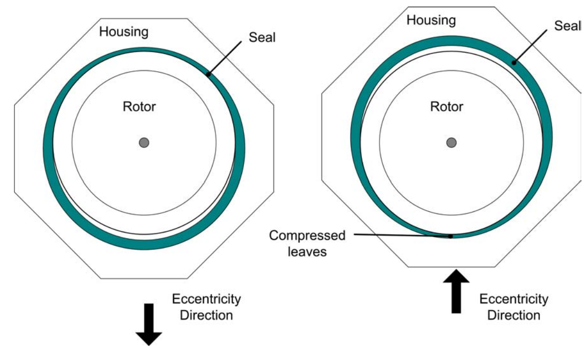

Figure 3. Facility operation

others. A number of potential sealing solutions can be grouped as compliant contacting seals. Here a compliant barrier is created between the stator and rotor, which generally is in contact with the rotor. During growth or excursions of the rotor, this compliant barrier is able to move with the rotor, thereby ensuring that the leakage remains low and that neither the rotor nor the barrier elements are significantly abraded. The typical seals that fit into this group are brush seals, finger seals and leaf seals (Fig. 1).

In order for compliant filament seals to be viable technologies in gas turbines, they need to exhibit a low leakage which must be maintained throughout their operational life. To achieve the life requirement, the seals need to exhibit a low wear rate for all operating conditions they may be subjected to. Wear, especially during incursions, can be very damaging to seal performance, since excessive wear during these periods of operation can cause the seal to operate with a clearance. This results in increased leakage, which is a performance loss.

A tool to investigate seal behaviour during rotor growth and rotor incursions is the Slow-Speed Stiffness Test Facility at the University of Oxford. This test rig has been described in detail by Franceschini et al. [3] and results from testing brush seals and a leaf seal on this test rig have been reported previously by Jahn et al. [4]. As a reference, a schematic of the facility is given in Fig. 2 and Fig. 3. On this rig, a rotor rotating at 3 RPM, a speed sufficient to overcome static friction, is incurred into a pair of seals. By measuring the force required for a given incursion, it is possible to characterise how a seal performs during rotor growth or rotor incursions. In an ideal seal the contact force between the sealing elements and the rotor would not increase significantly during such an event.

Herein some results from tests on a leaf seal (Fig. 1) are described. These tests showed a phenomenon that can be termed *Negative Stiffness*. First the experimental results are presented and then the cause of this phenomenon is explained by the means of modelling the individual effects that contribute to the leaf-to-rotor contact force.

EXPERIMENT DESCRIPTION

For the experiment a pair of leaf seals is pressurised in the Slow-Speed Stiffness Test Facility and then the rotor is moved to an eccentric position. During such a movement, the seal leakage and the force exerted on the housing by the rotor is measured. These two measurements are used to characterise the seal.

The test campaign used a leaf seal, similar to the one described by Jahn et al. [4], a schematic for which is given in Fig. 1. The seal contained approximately 4400 superalloy leaves, which were attached at an angle of 62° relative to the radial so that a seal bore diameter of 280mm was obtained. The seals used the same coverplate arrangement settings for all tests. While the incursions were carried out, the seal pressure drop was maintained constant. The aim of this is to generate a number of force-displacement graphs, which give an insight in seal stiffness and can be used for seal comparison.

An incursion cycle, as used during the tests, is shown in Fig. 4. The movements were repeated 3 times to ensure that any hysteresis effects are captured and also to demonstrate that the measured data were repeatable.

In total 13 tests were carried out at 9 pressure levels, including several repeats. Table 1 lists the tests in the order they were performed.

RESULTS

Figure 5 shows the force versus displacement graph for the case with no air flow. Force has been normalised so that the difference between the maximum and minimum measure of force equals 2. The maximum positive force is slightly larger than the maximum negative force, which can be attributed to the seal be-

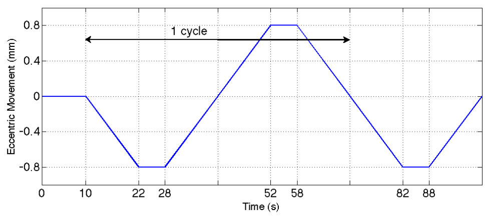

Figure 4. Displacement cycles used to characterise seal

Table 1. Incursion tests performed.

Test Index	P_U MPa	P_D MPa	Incursion mm
1	ambient	ambient	± 0.8
2	0.04	ambient	± 0.8
3	0.08	ambient	± 0.8
4	0.12	ambient	± 0.8
5	0.16	ambient	± 0.8
6	0.20	ambient	± 0.8
7	0.30	ambient	± 0.8
8	0.40	ambient	± 0.8
9	0.47	ambient	± 0.8
10	0.30	ambient	± 0.8
11	0.12	ambient	± 0.8
12	0.04	ambient	± 0.8
13	ambient	ambient	± 0.8

ing installed at a slightly eccentric position in the positive direction. The forces measured here correspond to the leaf mechanical stiffness of the seal. The gradient of the resulting line (force divided by displacement) can be defined as seal stiffness. For small incursions (less than ± 0.4mm), the seal stiffness is constant. For larger incursions the stiffness starts to increase, as the compliance limit of the leaf pack is approached.

Figure 6 shows an overlay of some force versus displacement plots obtained from the tests listed in Tab. 1. This graph shows two unexpected phenomena. First, seal stiffness reduces as a pressure drop is applied (0.08MPa compared to no air flow). This is opposite to the pressure stiffening effects that are typically seen in brush seals. Secondly, at higher pressures (> 0.08MPa) the stiffness actually becomes negative, meaning that once the rotor has been displaced from its central position, forces act on it in such a direction as to to pull it to a more eccentric position.

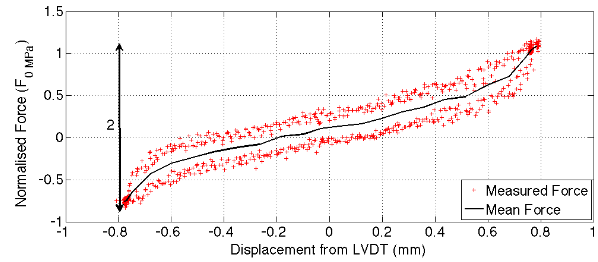

Figure 5. Force displacement cycle for case without air flow.

During each test the upstream pressure was constant and only small changes in mass flow rate were seen.

Figure 7 shows the force versus displacement graph corresponding to test 6 conducted at 0.20MPa. It is evident that for small incursions (± 0.4mm), the seals exhibit a negative but constant stiffness. Only for larger incursions ($> \pm 0.6$mm) does the stiffness become positive. Comparing Fig. 5 and Fig. 7, it is evident that the change in stiffness seen for large incursions at 0.20MPa corresponds to the stiffening also seen in the no air flow case for large incursions. This means that this effect can be attributed to a change in mechanical compliance of the leaf pack at large incursions.

Consequently, in order to obtain the negative stiffness, a force is required to act on the rotor and casing in addition to the mechanical leaf stiffness force. The graphs suggest that this force increases with pressure and also increases linearly with rotor-to-seal eccentricity.

Figures 8 and 9 show the displacement and force against time traces respectively. From these it is evident that there is a discontinuity in the force plots prior to the maximum excursions being reached ($t = 239, 244, 251\ldots$s). This is caused by the spring like properties of the load cell used in the test rig. At an eccentric point (e.g. $t = 242$s in Fig. 9), the load cell is loaded as the negative stiffness force pulls the rotor to an eccentric position. Subsequently, as the casing is moved toward the opposite extreme, the concentric position is traversed. At this point the load cell is unloaded and loaded in the opposite direction, resulting in a casing movement due to the spring like characteristic of the load cell. This sudden movement causes the discontinuities in the force trace. This could also be viewed as the backlash of the load cell.

The repeat tests (10 to 13) demonstrated very good repeatability of the observed force versus displacement traces.

LEAF SEAL MODEL

To understand the cause of the negative stiffness effect, a simplified seal model has been created. For this model, the leaf-rotor contact force is split into three main components. First there is the mechanical leaf stiffness; this is the force required

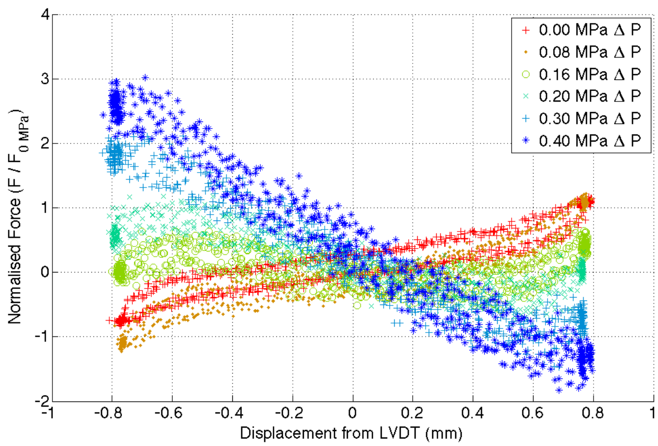

Figure 6. Composition of force-displacement cycles at different pressures (intermediate pressures have been omitted for clarity).

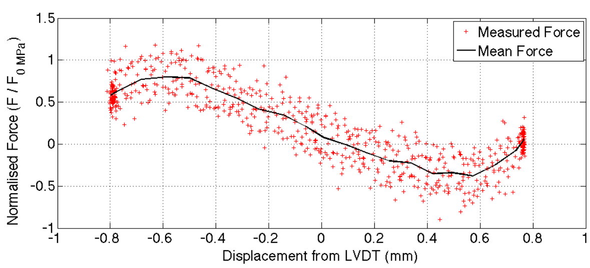

Figure 7. Force versus displacement plot at 0.2MPa (test 6).

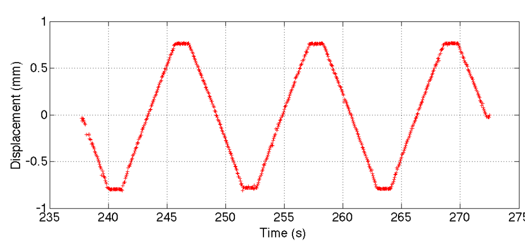

Figure 8. Incursion cycle applied at 0.2MPa.

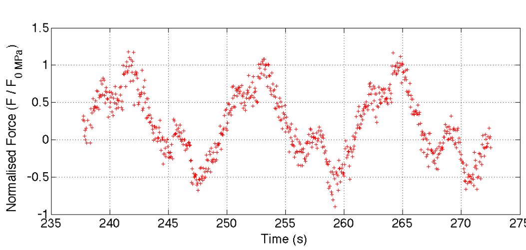

Figure 9. Measured force corresponding to movement cycle in figure 8.

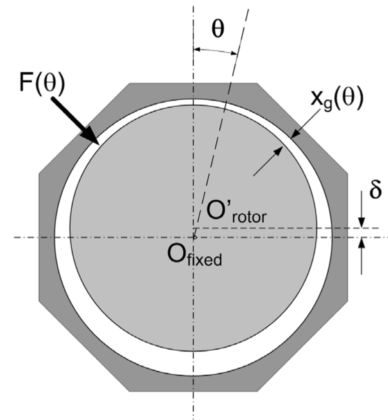

Figure 10. Eccentric rotor schematic.

to overcome the mechanical stiffness of the leaf pack, which is measured during incursions without air flow. Secondly there is a contribution from the pressure distribution within the leaf pack, which generally results in a blow-down force which increases with pressure drop. Finally there is a contribution due to the inertia change taking place as the flow enters the leaf pack. This is usually a lift-up force as described by Jahn et al. [4] and Franceschini et al. [5]. The magnitude of this third force is dependent on the coverplate geometry and the mass flow rate through the seal.

For small displacements ($|\delta| \leq 0.5mm$) these forces can be represented by linear approximations given as:

$$F_{Stiffness} = F_S = p_1\delta \tag{1}$$

$$F_{Pressure} = F_P = q_1 x_g + q_0 \tag{2}$$

$$F_{Inertia} = F_I = r_1 x_g + r_0 \tag{3}$$

where δ and x_g are the rotor eccentricity and coverplate to rotor gap and the remaining variables are the respective constants (see Fig. 10).

These forces either vary with rotor eccentricity δ or are linked to the coverplate to rotor gap, which depends on the local incursion. For a generic case, in which the rotor is displaced by the distance δ as shown in Fig. 10, the resulting coverplate to leaf gap is described by

$$x_g = x_0 - \delta\cos(\theta), \tag{4}$$

where x_0 is the coverplate to rotor gap corresponding to a central rotor.

Similarly by resolving in the direction of the eccentricity it can be shown that the net force contribution per leaf from the contact force is given by

$$F_\theta = F\cos(\theta), \tag{5}$$

which can be summed to give the net force

$$
\begin{aligned}
F_{Net} &= \sum_{\theta=0,\frac{2\pi}{N},2\frac{2\pi}{N},\ldots}^{2\pi} F_\theta \\
&= \sum_{i=1}^{N} F\cos\left(\frac{i2\pi}{N}\right)
\end{aligned}
\tag{6}
$$

where N is the total number of leaves and F is the contact force per leaf.

As the stiffness of the seal can be determined empirically, the stiffness force is included as a total force per seal ring rather than a force per leaf. Hence the total force acting on a seal can be given as

$$
\begin{aligned}
F_T &= F_S + F_{Net} \\
&= F_S + \sum_{i=1}^{N} F\cos\left(\frac{i2\pi}{N}\right) \\
&= F_S + \sum_{i=1}^{N} (F_P + F_I)\cos\left(\frac{i2\pi}{N}\right),
\end{aligned}
\tag{7}
$$

Substituting the expressions for F_S, F_I and F_P from Eqns. 1, 2 and 3 and by eliminating x_g with the expression in Eqn. 4 yields:

$$
\begin{aligned}
F_T = p_1\delta + \sum_{i=1}^{N} \Bigg[& q_1\left(x_0 - \delta\cos\left(\frac{i2\pi}{N}\right)\right) + q_0 \\
& + r_1\left(x_0 - \delta\cos\left(\frac{i2\pi}{N}\right)\right) + r_0 \Bigg] \cos\left(\frac{i2\pi}{N}\right)
\end{aligned}
\tag{8}
$$

This can be simplified to give:

$$
\begin{aligned}
F_T &= p_1\delta \\
&+ \sum_{i=1}^{N} (q_1x_0 + r_1x_0 + q_0 + r_0)\cos\left(\frac{i2\pi}{N}\right) \\
&- \sum_{i=1}^{N} (q_1\delta + r_1\delta)\cos^2\left(\frac{i2\pi}{N}\right)
\end{aligned}
\tag{9}
$$

Inspection of Eqn. 9 shows that the first summation term tends towards zero, as $\sum_{i=1}^{N}\cos\left(\frac{i2\pi}{N}\right) = 0$ for large N. Similarly it can be shown that $\sum_{i=1}^{N}\cos^2\left(\frac{i2\pi}{N}\right) = \frac{N}{2}$, if N is large.
Hence the stiffness relationship can be simplified to:

$$
\frac{F_T}{\delta} = p_1 - \frac{N}{2}(q_1 + r_1) \tag{10}
$$

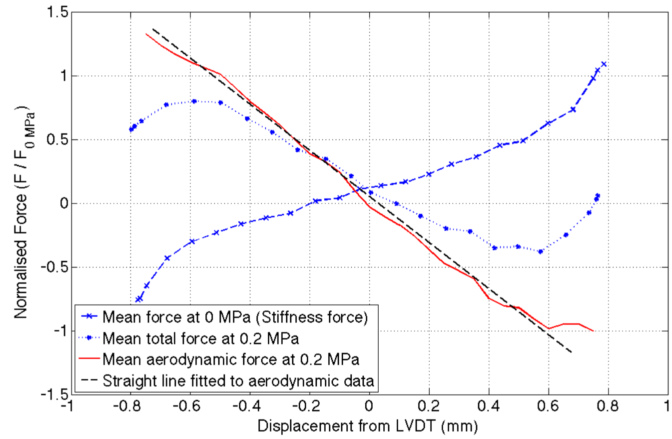

Figure 11. Difference in mean forces.

From this it can be seen that, depending on the magnitude and sign of the sum $(q_1 + r_1)$, the overall stiffness of the seal can be increased or decreased. Ultimately if $\frac{N}{2}(q_1 + r_1) > p_1$, the total force acting on the rotor for a positive displacement δ becomes negative. This is the requirement for negative stiffness. Effectively q_1 and/or r_1 need to be large and positive for negative stiffness to occur.

By putting positive values for q_1 and r_1 in Eqns. 2 and 3,

$$
\begin{aligned}
F_{Pressure} = F_P &= q_1x_g + q_0 \\
F_{Inertia} = F_I &= r_1x_g + r_0,
\end{aligned}
$$

it is evident that the forces F_P and F_I increase as the coverplate to rotor gap x_g increases. This means that the negative stiffness is caused by F_P and/or F_I being larger on the side of the rotor where the largest gap exists compared to the side with the smaller gap, meaning that the leaves are pushed more strongly against the rotor on the side with the large gap. This can be attributed to either increased blow-down on the side with the larger gap or increased lift-up on the side with the smaller gap. This means that the force exerted by the leaves on the rotor is affected by the local leaf pack geometry, the local coverplate to rotor gap and also the local leakage flow as these are the three parameters differing between the opposing sides of the seal.

This is in agreement with the models and the understanding published by Nakane et al. [6] and Franceschini et al. [5]. They show that the blow-down phenomenon is influenced by leaf pack geometry, mass flow rate through the seal and coverplate geometry.

Validation

The simple leaf seal model created previously suggests that seal stiffness is a simple addition of mechanical stiffness and stiffness related to aerodynamic forces and that, when the pressure is kept constant, the aerodynamic force is only a function of eccentricity. This hypothesis can be confirmed by subtracting the data given in Fig. 5 from the data given in Fig. 7. This is equivalent to subtracting the $p_1\delta$ term from Eqn. 10. The resulting graph is expected to show a straight line which corresponds to the $\frac{N}{2}(q_1+r_1)\delta$ term. Figure 11 shows the graph obtained by subtracting the mean stiffness of the no air flow graph (Fig. 5) from the graph obtained at 0.2MPa (Fig. 7). The resulting straight line confirms that the composition of the model is correct.

The increase in negative stiffness with pressure drop that has been observed in Fig. 6 suggests that the variables q_1 and r_1 are dependent on seal pressure. By repeating the above analysis, a relationship could be established.

DISCUSSION

The negative stiffness phenomenon described herein has several impacts on seal and sealing system operation. The main benefit of a seal with negative stiffness is that the leaf-rotor contact force decreases when the rotor is pushed into the seal as happens during rotor excursions or rotor growth. Consequently seal wear during these conditions is decreased.

A possible disadvantage is the force exerted on the rotor, which may affect rotor dynamics as the rotor effectively sees a force pushing it to a more eccentric position. Figure 6 shows that negative stiffness, and hence the force experienced, increases with pressure, meaning that this effect is likely to become significant at gas turbine operating conditions. A more in-depth study of this seals interaction with a high speed rotor is desirable.

SUMMARY AND CONCLUSION

Experimental results describing a negative stiffness effect seen in leaf seals have been presented. Under this effect a force acts on the seal rotor pushing it to an eccentric position. This force was observed to increase as the rotor eccentricity is increased. To understand the cause of this force, a simplified empirical leaf seal model was created in which the force was split into three contributors: leaf stiffness, a pressure related force and an inertia related force. The latter two and their interaction with the gap between coverplate and the rotor has been identified as the cause of the negative stiffness effect. Effectively the leaves experience more blow-down on the side where the gap increases and increased lift-up on the side where the gap decreases, resulting in a net force on the rotor which tends to push it into an eccentric position. Finally the experimental data have been used to validate the relationship between the forces used in the empirical model. It is possible that this negative stiffness effect could be present under certain conditions with other similar compliant filament seals such as brush seals. The condition that would be required is that the pressure or inertia force coefficients are large and positive as described.

ACKNOWLEDGMENT

This work was supported by Alstom Power Ltd and Rolls-Royce plc. The leaf seals were supplied by Alstom Power Ltd. The authors gratefully acknowledge the help and assistance provided by Paul Cooper, Dave Williams, Geir Leivseth, Nigel Rhodes and Terry Jones. The experimental apparatus was manufactured by Leo Verling. Their support is greatly appreciated.

REFERENCES

[1] Ferguson, J. G., 1988. "Brushes as high performance gas turbine seals". In Gas Turbine and Aeroengine Congress, ASME. 88-GT-182.

[2] Hendricks, R. C., Griffin, T. A., Kline, T. R., Csavina, K. R., Pancholi, A., and Sood, D., 1995. "Relative performance comparison between baseline labyrinth and dual-brush compressor discharge seals in a t-700 engine test". In International Gas Turbine and Aeroengine Congress and Exposition, ASME.

[3] Franceschini, G., Morgan, J. J., Jones, T. V., and Gillespie, D. R. H., 2006. "A slow-speed rotating test facility for characterising the stiffness of brush seals". In Gas Turbine and Aeroengine Congress, ASME. GT2006-91335.

[4] Jahn, I. H. J., Owen, A. K., Franceschini, G., and Gillespie, D. R. H., 2008. "Experimental characterisation of the stiffness and leakage of a prototype leaf seal for gas turbine applications". In Gas Turbine and Aeroengine Congress, ASME. GT2008-51206.

[5] Franceschini, G., Jones, T. V., and Gillespie, D. R. H., 2008. "Improved understanding of blow-down in filament seals". In Gas Turbine and Aeroengine Congress, ASME. GT2008-51197.

[6] Nakane, H., Maekawa, A., Akita, E., Akagi, K., Nakano, T., Nishimoto, S., Hashimoto, S., Shinohara, T., and Uehara, H., 2002. "The development of high performance leaf seals". In International Gas Turbine and Aeroengine Congress and Exhibition, ASME. 2002-GT-30243.